N-Deacetylases required for muramic-δ-lactam production are involved in *Clostridium difficile* sporulation, germination, and heat resistance

Received for publication, June 1, 2018, and in revised form, September 24, 2018 Published, Papers in Press, September 28, 2018, DOI 10.1074/jbc.RA118.004273

Héloise Coullon[‡1], Aline Rifflet[§¶], Richard Wheeler[§¶], Claire Janoir[‡], Ivo Gomperts Boneca[§¶], and Thomas Candela[‡2]

From the [‡]EA4043 Unité Bactéries Pathogènes et Santé (UBaPS), Université Paris-Sud, Université Paris-Saclay, 92290 Châtenay-Malabry, the [§]Institut Pasteur, Unité Biologie et Génétique de la Paroi Bactérienne, 75724 Paris, and [¶]INSERM, Équipe Avenir, 75015 Paris, France

Edited by Chris Whitfield

Spores are produced by many organisms as a survival mechanism activated in response to several environmental stresses. Bacterial spores are multilayered structures, one of which is a peptidoglycan layer called the cortex, containing muramic-δ-lactams that are synthesized by at least two bacterial enzymes, the muramoyl-L-alanine amidase CwlD and the *N*-deacetylase PdaA. This study focused on the spore cortex of *Clostridium difficile*, a Gram-positive, toxin-producing anaerobic bacterial pathogen that can colonize the human intestinal tract and is a leading cause of antibiotic-associated diarrhea. Using ultra-HPLC coupled with high-resolution MS, here we found that the spore cortex of the *C. difficile* 630Δ*erm* strain differs from that of *Bacillus subtilis*. Among these differences, the muramic-δ-lactams represented only 24% in *C. difficile*, compared with 50% in *B. subtilis*. CD630_14300 and CD630_27190 were identified as genes encoding the *C. difficile N*-deacetylases PdaA1 and PdaA2, required for muramic-δ-lactam synthesis. In a *pdaA1* mutant, only 0.4% of all muropeptides carried a muramic-δ-lactam modification, and muramic-δ-lactams were absent in the cortex of a *pdaA1–pdaA2* double mutant. Of note, the *pdaA1* mutant exhibited decreased sporulation, altered germination, decreased heat resistance, and delayed virulence in a hamster infection model. These results suggest a much greater role for muramic-δ-lactams in *C. difficile* than in other bacteria, including *B. subtilis*. In summary, the spore cortex of *C. difficile* contains lower levels of muramic-δ-lactams than that of *B. subtilis*, and PdaA1 is the major *N*-deacetylase for muramic-δ-lactam biosynthesis in *C. difficile*, contributing to sporulation, heat resistance, and virulence.

Clostridium difficile is a Gram-positive, spore-forming, toxin-producing anaerobic bacterium that can colonize the intestinal tracts of humans and other animals (1). *C. difficile* infection (CDI)[3] can lead to a spectrum of clinical signs, ranging from simple self-limiting diarrhea to life-threatening pseudomembranous colitis. Development of the infection has been linked to several risk factors, including antibiotic exposure and compromised immune systems (2). CDI is also associated with recurrent infections, which occur in 20–30% of patients who cleared a first infection (2). In health-care settings, *C. difficile* is considered the leading cause of antibiotic-associated diarrhea (3–5). The increase in cases led to the classification of *C. difficile* as an emerging infection by the World Health Organization (WHO) in 2009 (6). In fact, hospitalizations for CDI doubled from 2000 through 2010, and an estimated 450,000 cases of CDI occurred in 2011 in the United States. These increased rates and severity of CDI have been speculated to be a consequence of an enhanced *C. difficile* virulence (2, 7).

The pathophysiology of CDI is highly dependent on the sporulation and germination ability of *C. difficile*. Contamination results from the ingestion of spores, which can then reach the gastrointestinal tract. Upon alteration of the host microbiota, spores can germinate and produce vegetative cells. The vegetative cells are then responsible for colonization of the host, production of toxins, and induction of the range of symptoms associated with CDI. Vegetative cells finally sporulate, and spores are released in the environment through feces. Spores are therefore both the infectious and the persistence morphotype, responsible for the high dissemination rate of *C. difficile*. It has also been hypothesized that spore persistence in the gastrointestinal tract is a potential factor in the recurrences and relapses of CDI (2, 8). Moreover, a recent study has linked CotE, a spore coat protein, with host colonization, describing the spore as responsible for the initial colonization by targeting and binding the host mucus (9). Through their characteristics and contribution in pathophysiology, spores play a major role in CDI.

Spores are produced by many organisms as the result of a survival mechanism, triggered under several types of adverse

This work was supported in part by the French Government's Investissement d'Avenir Program, Laboratoire d'Excellence "Integrative Biology of Emerging Infectious Diseases," Grant ANR-10-LABX-62-IBEID. The authors declare that they have no conflicts of interest with the contents of this article.
This article contains Figs. S1–S6 and Tables S1–S6.
[1] Funded by Ministère de l'Enseignement Supérieur, de la Recherche et de l'Innovation.
[2] To whom correspondence should be addressed: EA 4043–Unité Bactéries Pathogènes et Santé, Université Paris Sud, 92296 Châtenay-Malabry, France. Tel.: 33-1-46-83-53-82; Fax: 33-1-46-83-55-57; E-mail: Thomas.candela@u-psud.fr.

[3] The abbreviations used are: CDI, *C. difficile* infection; TEM, transmission electron microscopy; BHI, brain heart infusion; CDMM, *C. difficile* minimal medium; SM, sporulation medium; SMC, sporulation medium C; Thi, thiamphenicol; CFU, colony-forming unit; SASP, small acid-soluble protein; UHPLC-HRMS, ultra-high-performance liquid chromatography–high-resolution mass spectrometry; DPA, dipicolinic acid.

environmental conditions. They are one of the most resistant life forms known, able to withstand heat, radiation, chemical exposure, desiccation, as well as treatment with many disinfectants (10). Such characteristics make for a remarkable persistence ability and contamination potential, and therefore they raise concerns in many sectors of human activities, such as the food industry or health care, and even more so with pathogenic bacteria.

Spores are multilayered structures, composed of a compressed dehydrated inner core, surrounded by the inner membrane, a germ cell wall, a peptidoglycan layer known as the cortex, an outer membrane, a proteinaceous external coat, and for some species the outermost layer called the exosporium. Many resistance characteristics of spores have been linked to this specific structural organization (10–12). Indeed, previous studies linked the coat with resistance to reactive chemicals such as oxidizing agents and disinfectants (13, 14). The dehydration level of the spore core and its high dipicolinic acid (DPA) and small acid-soluble protein (SASP) contents has been linked with heat resistance and DNA protection against radiations and chemical exposure (15). One of the spore specific structures is the thick peptidoglycan layer of the cortex.

The cortex structure has been studied in relatively few organisms, and mostly in *Bacillus*. The structure of the spore cortex has been published for *Bacillus subtilis* (16) and referenced as similar to the spore cortex of other *Bacillus* species, such as *Bacillus anthracis*. In *Clostridium* species, two studies analyzed spore cortex composition, using *Clostridium perfringens* and *Clostridium botulinum* (17, 18). Spore cortex shows several differences compared with vegetative cell peptidoglycan. In *B. subtilis*, muropeptides of the spore cortex carry either a cyclic muramic acid (muramic-δ-lactam), a tri- or tetrapeptide stem, or a single L-alanine residue, accounting for 50, 25, and 25%, respectively, of all muropeptides (16). Although muramic-δ-lactams also accounted for nearly 50% of all muropeptides in *C. perfringens*, single L-alanine residues were not identified in the spore cortex. Instead, tri- and tetrapeptide side chains represented over 45% of all muropeptides, and approximately 3% of all muropeptides carried no peptide side chain or δ-lactam ring. Another specificity of spore cortex is a low cross-linking index (11 and 2% in *B. subtilis* (16) and *C. perfringens* (18), respectively) compared with the vegetative cell.

In *B. subtilis,* muramic-δ-lactams have been described to be the result of a three-step process (19). The first step is the cleavage of the peptide on a muramic acid by a muramoyl-L-alanine amidase (CwlD) (20), followed by *N*-deacetylation of the muramic acid by the *N*-deacetylase PdaA (19). The muramic-δ-lactam ring would then be formed by a transpeptidase. CwlD and PdaA are essential for muramic-δ-lactam synthesis (21). In *B. subtilis*, disruption of any of these enzymes led to the complete disappearance of muramic-δ-lactams in the cortex and a strict interruption of the germination process, due to lack of cortex hydrolysis (22). However, mutants lacking either CwlD or PdaA are able to produce normal endospores, indicating that muramic-δ-lactam is not required for *B. subtilis* sporulation (22). These enzymes are well-described for *B. subtilis* (19, 20, 23) and *Bacillus thuringiensis* (24), but they have yet to be identified in any of the *Clostridium* species and particularly in *C. difficile.*

Given the notable rising concerns in health care settings, more and more studies are being conducted on *C. difficile* sporulation–germination mechanisms and host–pathogen interactions. Interestingly, an increasing number of studies have revealed significant differences between *C. difficile* and *B. subtilis* in sporulation and germination (25–27). A highly unique structure was described for the vegetative cell peptidoglycan of *C. difficile*, including a high level of *N*-deacetylation (28), and its impact on host–pathogen interactions. In contrast, we focused on the cortex *N*-deacetylases. Here, we provide the characterization of CD630_14300, renamed *pdaA1,* as the major *N*-deacetylase responsible for muramic-δ-lactam synthesis in *C. difficile*. Moreover, we also investigated the contribution of cortex structure to *C. difficile* virulence.

Results

C. difficile has an atypical cortex structure

Cortex from pure spore samples were extracted and analyzed through UHPLC (ultra-HPLC) coupled to HRMS (high-resolution MS), as described under "Experimental procedures." This analysis of the 630Δ*erm* spores constitutes the first detailed analysis of the cortex structure of *C. difficile* (Fig. 1). The complete list of all muropeptides detected, their area, and the calculated relative abundance can be found in Table 1 and Table S1, and the calculated parameters are detailed in Table S2. The vast majority of muropeptides detected in the analysis of the 630Δ*erm* parental strain were monomers (90.23% of all muropeptides), with only 9.77% of dimers and no detectable trimers. These results give a cross-linking index of 4.9%. Muramic-δ-lactams accounted for 24% of all muropeptides. Although tetrapeptides were the most frequent stem peptide encountered (43.5% of all muropeptides), the analysis surprisingly showed that 21.9% of muropeptides were not substituted with a stem peptide of any kind, not even with the single L-alanine as described in *B. subtilis* (16). The remaining muramic acid residues carried either a tripeptide or dipeptide stem peptide (4.8 and 5.8%, respectively). Additionally, 54.7% of muropeptides were *N*-deacetylated on the glucosamine residue. Overall, these results suggest that the *C. difficile* spore cortex is different compared with other published cortex analyses.

Identification of the PdaA N-deacetylase candidates

In *B. subtilis,* the *N*-deacetylase PdaA has been described as responsible for the second step of muramic-δ-lactam synthesis (19). To identify which of the 12 putative *N*-deacetylases of *C. difficile* were closest to *B. subtilis* PdaA, a multiple alignment was performed using Clustal Omega (29). In these alignments, two potential *N*-deacetylases of *C. difficile* were the closest to *B. subtilis* PdaA: CD630_14300 and CD630_27190 with 36.7 and 34.7% identity, respectively (Table S3). Both *C. difficile* *N*-deacetylases shared a very high similarity (40.7% identity) with each other and were selected as potential candidates in our study. Using the localization tool PSORT (30), CD630_27190 had a prediction for an internal helix, no signal peptide (PSORT (30)), and a potential membrane lipoprotein lipid attachment site (PROSITE (31)). Given these predictions, the CD630_27190 protein could be

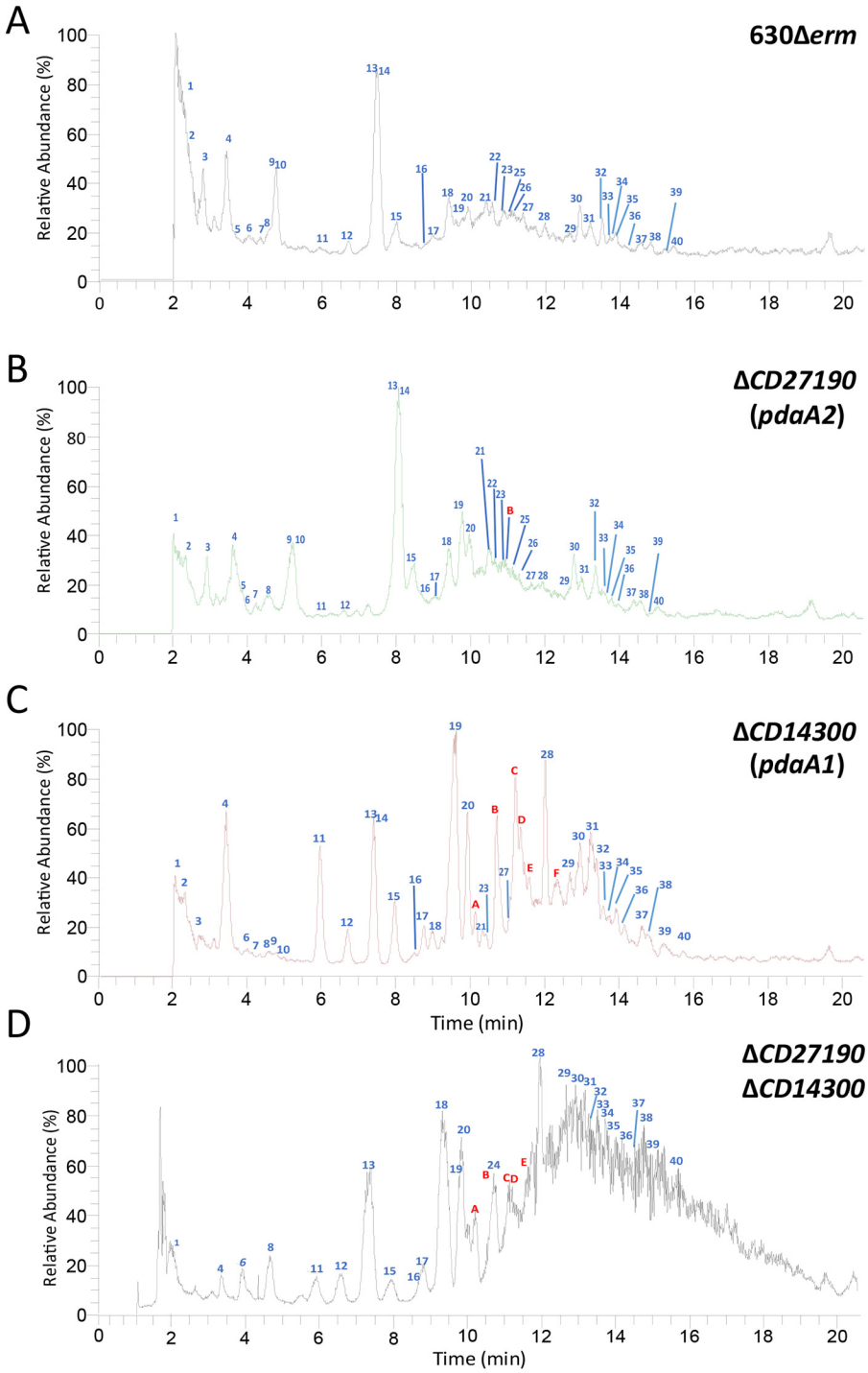

Figure 1. Muropeptide analysis of spore peptidoglycan by HRMS-coupled UHPLC. *A–D*, relative abundance (%) of muropeptides for the 630Δ*erm* strain (*A*), ΔCD630_27190 (*B*), ΔCD630_14300 (*C*), and double ΔCD630_14300ΔCD630_27190 (*D*) mutants. *Numerical peaks* refer to peaks identified in the parental strain. *Alphabetical peaks* refer to new peaks identified in the mutant profiles. Peak identification refers to Table 1.

membrane-associated, either in the vegetative cell membrane, facing the cytoplasm, or in one of the spore membranes. CD630_14300 was predicted to have both an internal helix and a signal peptide, giving a prediction of both cell wall–associated and extracellular localization of the protein, which is consistent with a spore cell wall–associated protein. To test our hypothesis, CD630_14300 and CD630_27190 were both investigated in *in vitro* experiments.

PdaA1 and PdaA2 are the N-deacetylases responsible for muramic-δ-lactam synthesis

To identify the *B. subtilis* PdaA ortholog in *C. difficile*, the cortex of both mutant strains was analyzed (Table 1 and Tables S1 and S2). The CD630_27190 spore cortex was similar to the parental profile, with the exceptions of the appearance of a single *N*-deacetylated hexasaccharide (peak B, representing 0.21% of all muropeptides) and a slight decrease in *N*-deacetylation

Table 1

Muropeptides detected in the cortex analysis of 630Δ*erm*, ΔCD630_14300, ΔCD630_27190 and ΔCD630_14300 ΔCD630_27190 strains

The following terms and abbreviations are used: ΔCD14300, CD630_14300; ΔCD27190, CD630_27190 cortex; GM, Glc*N*Ac-Mur*N*Ac; RT, retention time; deAc, *N*-deacetylation of the glucosamine; deAcX2, number of *N*-deacetylated glucosamine; Tri, disaccharide-tripeptide; Tetra, disaccharide-tetrapeptide; Gly, glycine; ND, not detected in the profile; NI, not identified with the fragmentation profile; gray cells, peaks for which precursor ion was not abundant enough to allow for fragmentation. Tri and tetra contain E-mDAP. The charge z is indicated in Table S1. Percentage of each peak was calculated as the ratio of the peak area over the sum of areas of all the peaks identified in the table.

Peak	Muropeptide	RT	Expected	Measured	Percentages			
			m/z	m/z	630Δ*erm*	ΔCD14300	ΔCD27190	ΔCD14300 ΔCD27190
1	Tetrapeptide missing GM	2.28	462.21945	462.21945	9,47	3,92	4,98	0,13
2	Tetrasaccharide (open lactam) deAc	2.42	440.20006	440.2002	0,74	0,02	0,39	ND
3	Tetrasaccharide (Reduced muramic lactam) deAc	2.77	431.19478	431.19531	6,49	0,25	4,04	ND
4	GM	3.4	499.21337	499.21387	8,25	9,69	10,81	1,49
5	Tetrasaccharide (Open lactam)-Tetrapeptide deAcX2	3.62	427.53282	427.53366	0,92	ND	1,23	ND
6	GM Tripeptide deAc	3.93	415.1864	415.1881	0,55	0,27	0,96	2,48
7	Tetrasaccharide (Open lactam)	4.26	461.20534	461.20618	0,75	0,03	1,47	ND
8	GM Tetrapeptide Gly	4,6	443.6980	443.6985	0,96	0,41	0,69	1,00
9	Tetrasaccharide (Reduced muramic lactam)-Tetrapeptide deAcX2	4.72	421.52929	421.52951	5,92	0,04	4,61	ND
10	Tetrasaccharide (Reduced muramic lactam)	4.72	452.20006	452.2003	5,27	0,24	5,55	ND
11	Tetrasaccharide deAc	5.91	468.19498	468.19614	0,82	6,76	1,15	2,02
12	GM Dipeptide deAc	6.65	657.2811	657.28381	2,28	3,94	2,79	3,11
13	GM Tetrapeptide deAc	7.38	450.70585	450.70566	16,01	13,66	14,30	17,49
14	Tetrasaccharide (Reduced muramic lactam)- Tetrapeptide deAc	7.47	652.79559	652.79578	19,08	0,06	17,98	ND
15	Hexasaccharides deAcX2	7.96	686.27963	686.28064	0,18	3,11	0,28	1,01
16	Octasaccharides deAcX3	8.71	603.2453	603.2463	0,09	1,62	0,13	0,42
17	GM Dipeptide	8.92	699.29307	699.29486	2,62	3,05	3,37	2,83
18	GM Tetrapeptide	9.4	471.7102	471.7119	2,56	4,22	3,58	8,93
19	Tetrasaccharide	9.53	489.20026	489.202	1,35	8,28	2,32	5,15
20	Tetrasaccharide-Tetrapeptide deAcX2	9.89	446.19609	446.1976	1,09	7,16	0,49	7,57
A	Tetrasaccharide-Dipeptide deAcX2	10.07	547.22955	547.23035	ND	1,56	ND	1,29
21	Tetrasaccharide (Reduced muramic lactam)- Tetrapeptide	10.37	673.8009	673.8033	2,40	0,02	3,41	ND
22	Tetrasaccharide (Reduced muramic lactam)-Dipeptide	10.53	552.2399	552.2419	0,62	ND	0,94	ND
23	Hexasaccharide (Reduced muramic lactam)_01	10.52	691.29	691.2933	0,64	0,15	1,05	ND
B	Hexasaccharides deAc_01	10.66	707.28491	707.2856	ND	1,82	0,21	0,85
24	Tetrasaccharide-Tetra deAC_01	10,76	689.7958	689.7961	0,00	2,51	0,00	5,93
25	Hexasaccharide (Reduced muramic lactam)_02	10.84	691.29	691.2933	0,80	ND	1,15	ND
26	NI	10.89	ND	729.6561	0,19	ND	0,21	ND
C	Octasaccharides deAcX2_01	11.17	617.2488	617.24921	ND	3,17	ND	0,67
D	Hexasaccharides deAc_02	11.31	707.28491	707.28601	ND	5,94	ND	2,06
27	NI	11.35		729.6561	0,25	ND	0,29	ND
E	Octasaccharides deAcX2_02	11.55	925.3696	925.3709	ND	0,50	ND	0,35
28	Tetrasaccharide-Tetrapeptide deAC_02	11.98	689.79578	689.7987	0,73	9,85	1,47	12,08
F	NI	12.27		815.326	ND	0,87	ND	ND
29	Tetrasaccharide-Tetrapeptide	12.81	710.80106	710.8016	0,16	0,97	0,49	4,95
30	GM Tripeptide + GM Tetrapeptide deAcX2_01	12.88	570.922	570.92438	3,22	1,98	3,92	5,27
31	Tetrasaccharide-Tetrapeptide + GM Tripeptide deAcX3_01	13.15	537.48625	537.4879	0,55	0,38	0,47	0,47
32	GM Tripeptide + GM Tetrapeptide deAcX2_02	13.49	570.92281	570.92517	2,97	1,31	3,12	3,87
33	GM Tetrapeptide + GM Tetrapeptide deAcX2	13.58	594.60185	594.6047	0,34	0,37	0,36	0,83
34	Tetrasaccharide-Tetrapeptide + GM Tri peptide deAcX3_02	13.68	537.48625	537.4879	0,45	0,22	0,36	0,38
35	GM Tripeptide + GM Tetrapeptide deAc_01	13.85	876.8867	876.8891	0,26	0,40	0,29	0,99
36	GM Tetrapeptide + GM Tetrapeptide deAcX2_02	14.11	594.60185	594.6047	0,38	0,36	0,39	0,77
37	GM Tripeptide + GM Tetrapeptide deAc_02	14.48	876.88586	876.8891	0,15	0,11	0,16	0,50
38	Tetrasaccharide-Tetrapeptide + GM Tripeptide deAcX2_01	14.68	730.3161	730.3197	0,29	0,51	0,34	0,85
39	GM Tripeptide + GM Tetrapeptide	15.08	897.89114	897.8958	0,03	0,13	0,05	0,32
40	Tetrasaccharide-Tetrapeptide+ GM Tri peptide deAcX2_02	15.21	730.3161	730.3197	0,17	0,14	0,20	0,41

level (49.1% compared with the 54.8% of the parental strain). Other parameters remained similar, including the relative abundance of muramic-δ-lactams.

However, cortex analysis of CD630_14300 mutant spores revealed striking differences relative to the parental cortex. The most notable variation was the disappearance of five peaks, all of which were muropeptides carrying muramic-δ-lactams. Similarly, five additional peaks suffered a strong decrease in relative abundance, producing no detectable precursor ion for fragmentation analysis (gray cells in Table 1). The measured masses (*m*/*z*) of these muropeptides were compatible with structures carrying muramic-δ-lactams. Taken together, these variations are responsible for a drastic decrease in muramic-δ-lactam content: only 0.4% of all muropeptides carry a muramic-δ-lactam modification, whereas 24% of muropeptides carried muramic-δ-lactams in the parental spore cortex. In the CD630_14300 mutant, dimers represented a lower relative amount than in the parental profile (6.20% *versus* 9.77%), and the corresponding cross-linking index was decreased in the CD630_14300 mutant (3.10% *versus* 4.90%). Furthermore, the most frequent muropeptides in the CD630_14300 mutant were not tetrapeptides, as detected in the parental strain, but saccharides carrying neither stem peptide nor muramic-δ-lactam ring. In the CD630_14300 mutant, these muropeptides represented 55.4% of all muropeptides. The CD630_14300 cortex analysis also revealed peaks previously absent from the parental strain, which corresponded to hexasaccharides and octasaccharides carrying various degrees of *N*-deacetylation. In our analysis, hexasaccharides and octasaccharides represented a higher relative abundance in the CD630_14300 mutant (11.6 and 5.6% of all muropeptides, respectively, compared with 1.80 and 0.10% in the parental strain). These results suggest that CD630_14300 is the major *N*-deacetylase responsible for muramic-δ-lactam synthesis and was therefore renamed *pdaA1*.

The double mutant ΔCD630_14300 ΔCD630_27190 was also constructed. In this mutant, cortex analysis revealed striking differences relative to the parental cortex. The major difference was the total absence of muramic-δ-lactams in the double mutant spore cortex. This result suggests that CD630_27190 is the second *N*-deacetylase responsible for muramic-δ-lactam synthesis and was therefore renamed *pdaA2*. As seen with the CD630_14300 mutant, the abundance of unsubstituted muropeptides is increased in the profile obtained for the double mutant (30.7% of all muropeptides, compared with 21.9% for the parental strain).

Spores lacking muramic-δ-lactam undergo a delayed germination

Given the role of muramic-δ-lactam residues in spore germination (22), the *in vitro* germination of *pdaA1* mutant spores was investigated. Spores of the parental 630Δ*erm* strain showed a quick $OD_{600\,nm}$ decrease of about 10% within 10 min, followed by a plateau for the remaining 50 min (Fig. 2*A*). In comparison, the *pdaA1* mutant showed a slight but reproducible progressive increase in optical density, reaching 3% at 10 min. The kinetics of DPA release was also examined, and DPA was not released from the spores of the *pdaA1* mutant, in contrast to the parental and the complemented strains (Fig. S1*A*). To assess whether *pdaA1* mutant spores could undergo germination altogether, the monitoring assay was extended to 24 h (Fig. 2*B*). In this extended monitoring, after 24 h, parental spores showed a very slow continuous decrease in optical density reaching 80% of the initial $OD_{600\,nm}$, and spores lacking PdaA1 showed a slow decrease in $OD_{600\,nm}$, reaching 90% of the initial $OD_{600\,nm}$. In both monitoring assays, the spores of the *pdaA1* complemented strain showed a profile of optical density similar to the parental spores.

Because colonies of the *pdaA1* mutant were formed after spore plating, germination was investigated using a solid medium incubated for 48 h. Colonies of the parental and *pdaA1* mutant strains were examined at 24 and 48 h incubation. Visual examination of both strains showed a strong difference in colony size at 24 h (Fig. 2, *C–D*, Student's *t* test, $p = 6.6E\text{-}11$). Colonies of the parental strain were small but clearly visible (average of 2 mm in diameter, Fig. 2*C*), whereas *pdaA1* colonies were barely visible (average of 1 mm). However, colonies no longer showed this difference after 48 h incubation as both strains had an average diameter of 6 mm (Student's *t* test, $p = 0.99$). These results suggest that *pdaA1* deletion induces a significant delay in germination but does not block the process altogether. Moreover, in a liquid culture, the *pdaA1* mutant showed no growth defect compared with the parental strain (Fig. S2). This result suggests that the colony phenotype observed at 24 h incubation is further evidence of a germination delay rather than a growth defect. In the complemented mutant, the germination ability is restored (Fig. S3). Taken together, the results suggest that the *pdaA1* mutant has an altered germination process.

The germination delay of the double mutant (*pdaA1* and *pdaA2*) was also examined at 24 and 48 h incubation. Similarly to the phenotype observed for the *pdaA1* mutant, this double mutant is still able to germinate (Fig. S3).

Spore morphology of the pdaA1 mutant

After identifying the cortex modifications and their impact on spore germination, cell morphology was investigated to determine whether such modifications would be associated with an altered spore structure (Fig. 3). To allow minimal disruption of spore structures, spore morphology was assessed through transmission EM (TEM) examination of sporulating cultures obtained with liquid SMC broth and minimal purification steps. Examination of the parental strain micrographs showed the spore structures, as described previously (32): an exosporium, the outer and inner coat, outer membrane, cortex, inner membrane, and core (Fig. 3*A*). TEM analysis of *pdaA1* mutant spores did not reveal significant differences in spore structure between the parental and *pdaA1* mutant strains (Fig. 3, *A* and *B*). However, for the *pdaA1* mutant spores, the membranes and interfaces of the internal structures appeared blurred and undefined regardless of the focal planes scanned. These observations are particularly visible for the inner and outer membranes. The significance of such a phenotype has yet to be understood.

Overall, examination of sporulating cultures revealed that endospores were less frequent in the *pdaA1* mutant compared

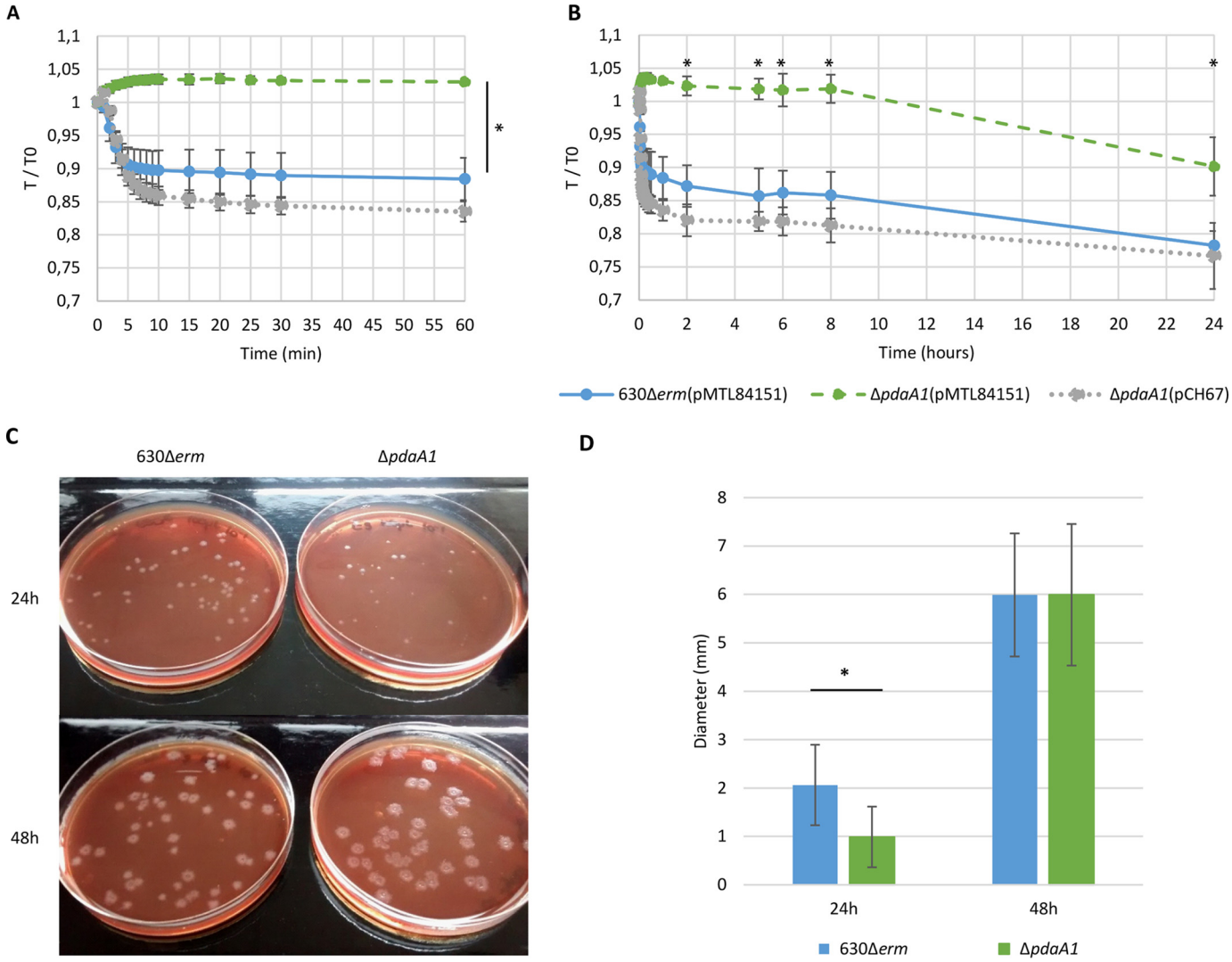

Figure 2. Spores lacking muramic-δ-lactam undergo a delayed germination. Spore germination was monitored for the optical density assay at 600 nm after the addition of 0.1% sodium taurocholate in BHISG, for 60 min (*A*) or 24 h (*B*), for the 630Δ*erm*(pMTL84151) parental strain in *blue*, Δ*pdaA1*(pMTL84151) strain in *green*, and the complemented *pdaA1* mutant strain (Δ*pdaA1*(pCH67)) in *gray*. Results are expressed as the ratio of $OD_{600\ nm}$ observed at time point (*T*) over the initial $OD_{600\ nm}$ at $T = 0$ (*T0*). Assessment of germination delay in solid BHI supplemented with horse blood and taurocholates was performed for the 630Δ*erm* and the Δ*pdaA1* strains (*C*). Colony sizes were measured (*D*) and presented in *blue* for the 630Δ*erm* strain and in *green* for the Δ*pdaA1* strain. *, Student's *t* test, $p < 0.005$. Results are expressed as the average values and standard deviations of at least three independent experiments, except for the assessment of germination delay in solid BHI (*C*) which is representative of three independent experiments.

with the parental strain (22% *versus* 55% of cells). Moreover, 79% of *pdaA1* endospores showed an altered morphology (coat detachment or membrane defect), compared with 8% in the parental strain. In addition, the *pdaA1* strain produced a higher amount of debris (Fig. S4). Such structures could represent empty spores, detached structures from abnormal spores, or remnants of aborted endospores, suggesting a potential assembly defect in *pdaA1* mutant spores (Fig. S4, *black arrows*).

Modification of cortex structure increases wet heat sensitivity

Because TEM experiments on sporulating cultures suggested a potential anomaly in spore assembly, they were subsequently repeated on pure spore suspensions to allow for measurements and statistical analysis of spore morphology (Fig. 4*A* and Fig. S5). Although external structures could be focused on, scanning focal planes did not produce clear limitations of internal structures, particularly the membranes and interfaces, as already observed for TEM on sporulating culture. TEM representative images of *C. difficile* spore cross-sections are included in Fig. S5, *A–D*. The results obtained for longitudinal sections can be found in Fig. 4*A*, whereas full results are detailed in Fig. S5, *table*. In longitudinal sections, the core of *pdaA1* mutant spores was longer and wider on average than the parental strain (1122 and 392.2 nm *versus* 912.9 and 230.6 nm, respectively, Student's *t* test, $p < 0.05$). The calculated core volume was three times greater for the *pdaA1* mutant strain compared with the parental strain (7.39×10^8 nm^3 *versus* 2.08×10^8 nm^3, Student's *t* test, $p < 0.05$). The thickness of the cortex layer was also investigated. In the *pdaA1* mutant spore longitudinal cross-sections, the cortex measured an average of 74.54 nm, whereas it only reached 34.17 nm for the parental longitudinal cross-sections. These results suggest that the cortex thickness is significantly increased in the *pdaA1* mutant spores, reaching twice the thickness of the parental spore cortex. All the param-

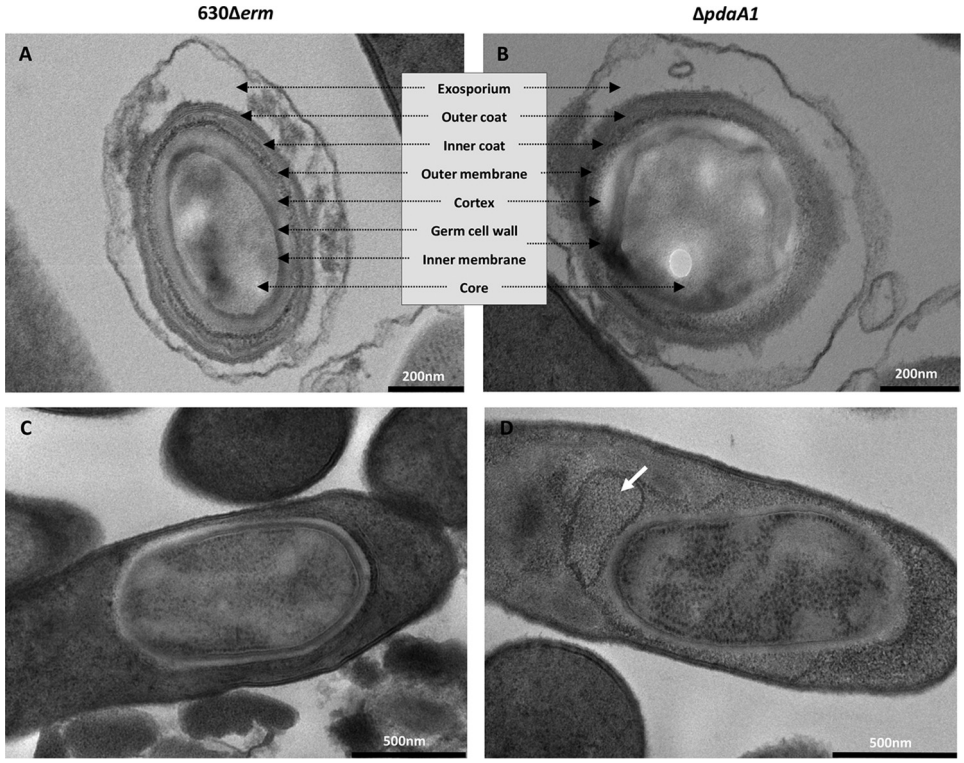

Figure 3. *pdaA1* mutant spore morphology. EM of 630Δ*erm* spores (*A*) and endospores (*C*) was compared with Δ*pdaA1* mutant spores (*B*) and endospores (*D*). The spore layers identified are indicated in the *inset* between *A* and *B*. The legends are indicated by the *bars* in the *bottom right corner*, representing 200 nm for the spores and 500 nm for the endospores. The *white arrow* indicates detached structures.

eters measured and calculated for the longitudinal sections follow a similar trend in the transversal sections (Fig. S5). Taken together, these results suggest that *pdaA1* mutant spores are larger, with an increased core volume (3-fold, $p < 0.05$), an increased cortex thickness (2-fold, $p < 0.05$), and a slightly decreased protoplast/sporoplast ratio ($p < 0.05$).

After validating the spore assembly and morphology phenotype in the *pdaA1* mutant strain, we sought to identify the potential consequences of such a phenotype on spore resistance characteristics. The chemical resistance of purified *pdaA1* mutant spores was therefore investigated (Fig. 4*B*) as described previously (14). Two chemicals, hydrogen peroxide and ethanol, frequently used in chemical resistance spore assays in *C. difficile*, were tested. In our experiments, *pdaA1* mutant spores had a similar log reduction of spore titers after ethanol or hydrogen peroxide treatment compared with the parental and complemented spores (Student's *t* test, $p > 0.05$). This result indicates that the defect in spore assembly for the *pdaA1* mutant does not significantly alter the chemical resistance properties of spores. Our results also suggest that ethanol treatment is an appropriate method for enumeration of *pdaA1* mutant spores in sporulating cultures.

Wet heat resistance has been linked to a large number of factors, including factors related to core structure (dehydration, DPA contents, and SASPs proteins (10)). Considering that the *pdaA1* mutant spores have an increased core volume compared with the parental strain, which suggests a decreased core dehydration, the heat resistance of purified *pdaA1* mutant spores was also investigated (Fig. 4*B*). After incubation at 65 °C for 20 min, spore suspensions of the *pdaA1* mutant strain suffered a greater log reduction compared with the parental and complemented strain (1.15 *versus* 0.37 and 0.47 logR, respectively). This suggests that the heat resistance of *pdaA1* mutant spores is slightly but significantly decreased compared with the parental and complemented strain (Student's *t* test, $p < 0.05$).

Modification of cortex structure reduces sporulation rate

Because the TEM experiment suggested a potential defect in spore assembly, sporulation percentages were investigated for the parental strain harboring the empty control plasmid pMTL84151, the *pdaA1* mutant harboring pMTL84151, and the complemented *pdaA1* mutant harboring pCH67, in sporulating cultures after 72 h (Fig. 5) as described previously (33). Given that the resistance assays indicate that the three strains have a similar resistance to ethanol treatment, enumeration of the relative abundance of spores and vegetative cells was conducted using heat-shock as well as ethanol treatment as a control (Fig. 5, *A* and *B*). The results of three independent biological replicates can be found for each strain and condition in Table S4. Total mean cell titers did not differ between the parental strain harboring the empty pMTL84151 plasmid (2.0×10^6 CFU/ml), the *pdaA1* mutant harboring pMTL84151 (2.3×10^6 CFU/ml), or the *pdaA1* complemented strain harboring the pCH67 plasmid (3.7×10^6 CFU/ml) ($p > 0.05$). In these sporulation studies, ethanol-resistant spores represented 37.2% (7.68×10^5 CFU/ml), 6% (1.53×10^5 CFU/ml), and 87.6% (3.11×10^6 CFU/ml) of the total cell titers for the parental strain, the *pdaA1* mutant, and the complemented mutant, respectively. These results suggest that the *pdaA1* mutant has a

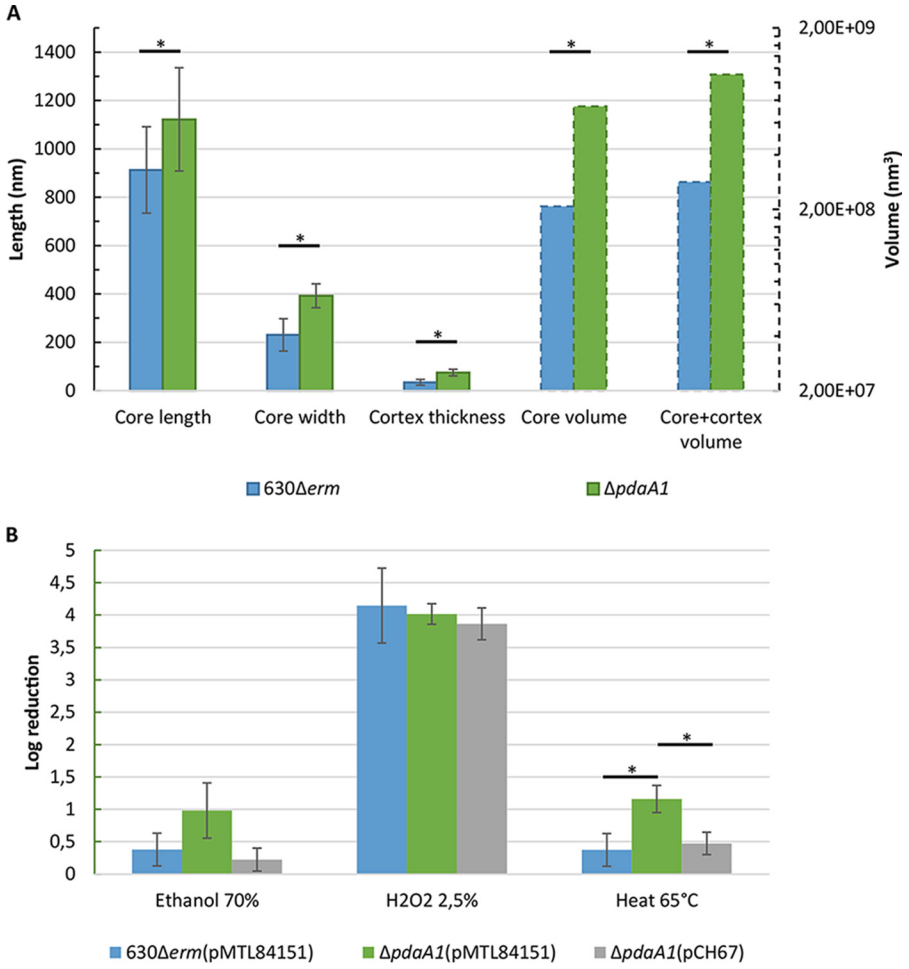

Figure 4. Modification of cortex structure and spore morphology does not alter chemical resistance. Spore measurements (*A*) were obtained for pure spore suspensions of the parental (*blue*) and *pdaA1* mutant strain (*green*). *Solid bars* indicate the measured length (*left axis*, nm), and the *dotted bars* indicate the calculated volumes (*right axis*, nm^3). Chemical and heat sensitivities of purified spore suspensions (*B*) were obtained for three independent biological replicates of pure spore suspensions: 630Δ*erm*(pMTL84151) spores in *blue*, Δ*pdaA1*(pMTL84151) spores in *green,* and the complemented mutant spores Δ*pdaA1*(pCH67) strain in *gray*. *, Student's *t* test, $p < 0.05$.

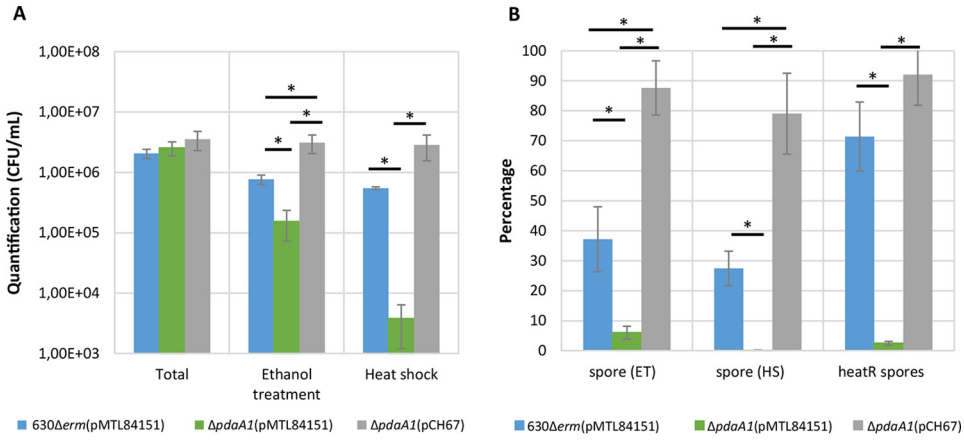

Figure 5. *pdaA1* mutant has a defect in sporulation and spore heat resistance. Quantification of sporulation titers after 72 h incubation in SM broth (*A*), percentage of spores recovered after ethanol treatment (*ET*), heat shock (*HS*), and heat-resistant spores ($heat^R$) (*B*) of 630Δ*erm*(pMTL84151) strain in *blue*, Δ*pdaA1*(pMTL84151) strain in *green,* and the complemented strain Δ*pdaA1*(pCH67) strain in *gray* are presented. Results are expressed as the average values and standard deviations of at least three independent experiments. *, Student's *t* test, $p < 0.005$.

reduced sporulation percentage compared with the parental strain ($p < 0.005$). The observed sporulation percentage of the complemented strain suggests that the sporulation defect is restored when complementing the *pdaA1* mutant with pCH67.

Heat-resistant spore titers were also counted for the strains, giving rise to different spore counts compared with ethanol treatment. Following 72 h of incubation, spore titers differed in a significant manner for the *pdaA1* mutant, whereas ethanol-

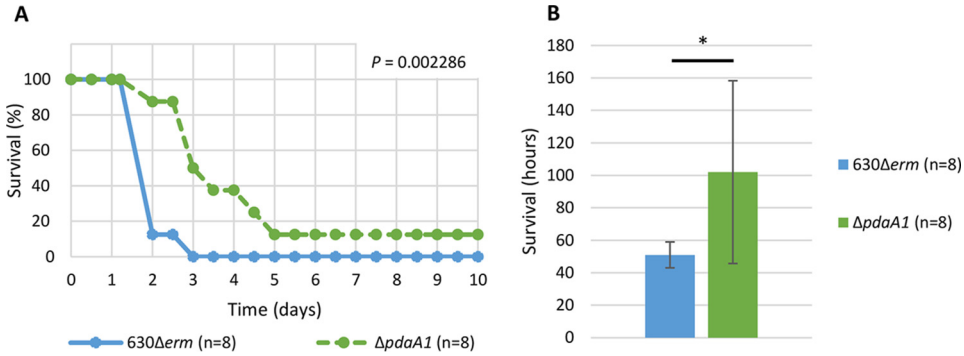

Figure 6. *pdaA1* mutant strain has a delayed virulence. Kaplan-Meier survival curve ($p = 0.002286$) depicts hamster survival (*A*) and average time to mortality (*B*) for the strain 630Δ*erm* in *blue* and Δ*pdaA1* mutant in *green*. *, Student's *t* test, $p < 0.005$.

resistant spores represented 6% of total cell titers (1.53×10^5 CFU/ml), heat-resistant spore titers barely reached 0.13% of total cells (3.8×10^3 CFU/ml). These results indicate that only 2.5% of spores produced by the *pdaA1* mutant are heat-resistant (Fig. 5*B*). In comparison, ethanol-resistant and heat-resistant spores represented 37.2% (5.48×10^5 CFU/ml) and 27.5% (7.68×10^5 CFU/ml) of total cell titers in the parental strain, which indicates that 71% of spores produced at 72 h are heat-resistant in the parental strain. Similarly, ethanol-resistant and heat-resistant spores produced by the complemented strain represented 87% (3.11×10^6 CFU/ml) and 79% (2.86×10^6 CFU/ml), respectively, of total cell titers. These results suggest that the *pdaA1* spores have a decreased heat resistance compared with the parental strain ($p < 0.005$), and the phenotype is restored in the complemented strain.

pdaA1 mutant has a delayed virulence

Because the germination timing of *C. difficile* may modulate the course of the infection process, the ability of the *pdaA1* mutant to cause illness in a hamster model of infection was tested (Fig. 6). After oral administration of spores, all hamsters were tested for the presence of *C. difficile* through an on/off detection method, and carriage of *C. difficile* was confirmed for both groups of hamsters. In our assay, all eight hamsters of the parental strain group were either deceased or euthanized between 2 and 3 days post-infection. In comparison, the hamsters infected with *pdaA1* mutant spores survived up to 5 days post-infection before reaching a similar mortality rate. One hamster in this group eventually cleared *C. difficile* from its gastrointestinal tract and survived throughout the assay (Fig. 6*A*). These results indicate that hamsters infected with the *pdaA1* mutant reached mortality significantly later than those infected with the parental strain (Fig. 6*B*, 51 ± 8 h and 102 ± 56 h, respectively, $p < 0.05$). These results indicate that the *pdaA1* mutant has a significantly delayed virulence compared with the parental strain (Kaplan-Meier log rank, $p = 0.002286$).

Discussion

Our analysis of *C. difficile* 630Δ*erm* spore cortex revealed an atypical structure compared with other species. In our analysis, muramic-δ-lactams were present on 24% of muropeptides, which is significantly less than the relative abundance found in other species (50% in *B. subtilis* and *C. perfringens*). We also determined the glucosamine *N*-deacetylation level of spore cortex: in the parental 630Δ*erm* cortex, approximately 55% of muropeptides are *N*-deacetylated on the GlcNAc residue (GlcNAc), which constitutes a surprising result in itself, contrasting with the previous published cortex structures (16, 18). Indeed, GlcNAc *N*-deacetylation was not reported at all in *B. subtilis*, and the cortex of *Bacillus megaterium* and *C. perfringens* showed a very low level of GlcNAc *N*-deacetylation (1% in *B. megaterium* (34) and 10% in *C. perfringens* (18)). These differences in cortex *N*-deacetylation are particularly surprising, given that all these genomes contain several potential *N*-deacetylases. Indeed, six *N*-deacetylases have been annotated in the *B. subtilis* genome (35). Analysis of *C. perfringens* and *B. megaterium* genomes using the IMG/JGI database (36) showed that these contained 8 and 13 potential *N*-deacetylases, respectively, based on the identification of a pfam01522 domain. Global levels of GlcNAc *N*-deacetylation in the spore cortex indicate that among the remaining potential 11 *N*-deacetylases of *C. difficile*, there is potentially one enzyme or more able to target this residue in spore cortex, which shows another specificity of *C. difficile* cortex compared with other species. The link between the number of potential *N*-deacetylases and *N*-deacetylation levels in spore cortex has yet to be investigated, and to our knowledge the specific impact of GlcNAc *N*-deacetylation in the spore cortex has not been studied in any species. The first evidence of the *N*-deacetylase activity on the spore cortex GlcNAc is the slightly decreased *N*-deacetylation noted in *pdaA2* mutant spore cortex. It is noteworthy that such modification induces no significant difference between the *pdaA2* mutant compared with the parental strain, either in sporulation rate or in germination (Fig. S6).

Additionally, our analysis of the *C. difficile* cortex also revealed a lack of muropeptides carrying a single L-alanine (25% of muropeptides in *B. subtilis*), but detected muropeptides carrying no stem peptide or muramic-δ-lactam modification, in a much higher relative abundance than the previous characterization in *C. perfringens* (2.4% of all muropeptides (18)). In *B. subtilis*, the single L-alanine muropeptides have been suggested by Popham *et al.* (22) to be intermediate states on the pathway to muramic-δ-lactam synthesis, but a precise mechanism has yet to be proposed. Similarly, the small amount of muropeptides carrying a MurNAc with no stem peptide in *C. perfringens* has also been suggested to be the result of intermediate steps of muramic-δ-lactam synthesis (20). In our anal-

ysis, these muropeptides carrying no stem peptide or muramic-δ-lactam represent a significantly higher relative abundance than the data published for *C. perfringens* (22% in *C. difficile versus* 2% in *C. perfringens* (18)). The higher relative abundance of muropeptides carrying a MurNAc with no stem peptide could have an impact on peptidoglycan properties: flexibility, sensitivity to lytic enzymes, protein binding, or osmotic properties. These results indicate that the *C. difficile* cortex structure is not only highly different compared with *Bacillus* species but also compared with other *Clostridium* cortex structures published as of today.

In a *C. difficile* mono-associated mice model, *pdaA1* was found to be up-regulated during infection (4.5- and 4.1-fold at 14 and 38 h post-challenge, respectively (37)) and is suggested to be strongly induced by σ^F and σ^G (38). Moreover, *pdaA1* represents the 14th most abundant mRNA in dormant spores (39). These results suggest that *pdaA1* is expressed both in early and late sporulation stages, with an increased expression during *in vivo* infection. The cortex analysis of the *pdaA1* mutant significantly differed from that of the 630Δ*erm* strain. The most striking result was the nearly complete disappearance of muramic-δ-lactams, representing 0.4% of all muropeptides in the *pdaA1* mutant and the complete disappearance in the double mutant *pdaA1–pdaA2* instead of 24% in the 630Δ*erm* strain. Synthesis of muramic-δ-lactams in *C. difficile* may follow similar steps as described for *B. subtilis*: cleavage by an amidase first (CwlD) (20), followed by *N*-deacetylation and cyclization of muramic-δ-lactam (19). PdaA1, and to a lesser extend PdaA2, would act as the *N*-deacetylase in the second step of the synthesis. As observed, their absence would lead to the accumulation of muropeptides carrying no stem peptide or δ-lactam ring (55.4% in the *pdaA1* mutant and 30.7% in the *pdaA1–pdaA2* double mutant *versus* 21.9% in the parental strain) as the consequence of CwlD cleavage of side chains. It could be argued that the germination delay of the *pdaA1* mutant is linked to the traces of muramic-δ-lactam still present in the cortex of the *pdaA1* mutant (0.4% of muropeptides). However, the cortex of the *pdaA1–pdaA2* double mutant has a complete lack of muramic-δ-lactams, and spores show a germination delay similar to the *pdaA1* mutant spores. The previous germination delay hypothesis may therefore be discarded.

In *B. subtilis*, the lack of muramic-δ-lactams blocked both the cortex hydrolysis and spore outgrowth, and proper germination could only be restored by a lysozyme-induced artificial cortex hydrolysis (20). Surprisingly, the lack of muramic-δ-lactams in *C. difficile* does not appear to induce the same interruption of germination. Instead of blocking germination altogether, lack of muramic-δ-lactam in *C. difficile* induced a strongly delayed and slowed germination process, and the artificial cortex hydrolysis was therefore not necessary in our experiments. The most likely hypothesis for such a difference could be that cortex lytic enzymes of *C. difficile* have a less stringent substrate specificity (41, 42).

Although muramic-δ-lactams have been largely accepted as targets of cortex lytic enzymes involved in the germination process, the latest studies in *B. subtilis* have linked muramic-δ-lactams with spore outgrowth but not heat resistance or spore dehydration (22). The findings in our study would suggest that muramic-δ-lactams in *C. difficile* spores may play a different role compared with *B. subtilis*. Indeed, in our TEM experiments, spore measurements indicated that although the ultrastructure of spores was globally conserved in the *pdaA1* mutant, lack of muramic-δ-lactams induced an increase in spore volume and cortex thickness, which in turn induced a larger spore. The increase in the heat sensitivity of Δ*pdaA1* mutant spores relative to parental spores was not due to decreased DPA levels, because measurement of spore DPA levels revealed that Δ*pdaA1* spores had slightly higher levels of DPA than parental spores, without reaching statistically significant values ($p > 0.05$, Fig. S1*B*). Interestingly, the yield of muropeptides from a similar amount of freeze-dried spores in our cortex analysis was comparable for the 630Δ*erm* and *pdaA1* mutant: similar weight of freeze-dried muropeptides during purification and similar total peaks area during UHPLC analysis (Table S5), which suggests that the amount of cortex is similar in both strains. This suggests that the difference of thickness between the *pdaA1* mutant and the parental spore cortex may be due to structural differences rather than the amount of peptidoglycan. We hypothesize that in *C. difficile* the lack of muramic-δ-lactams as a consequence of *pdaA1* deletion could induce a change in spore cortex organization. In turn, this alteration of cortex structure could induce a modification of its physical–chemical properties and may alter the spore dehydration process, giving rise to a larger and more hydrated core. Finally, these alterations would build up to the increased heat sensitivity.

To our knowledge, our study is the first to connect the sporulation process with muramic-δ-lactams. In TEM, our observations noted an increase in abnormal assembly in endospores, associated with the increase in empty round cells and debris. These results are consistent with the empty round cells observed in other studies (33), which have been correlated to an altered sporulation process. These results are also consistent with the observed sporulation defect of the *pdaA1* mutant (6% *versus* 37.1% sporulation percentage, respectively). Taken together, our findings suggest that muramic-δ-lactams and their synthesis influence the process of sporulation in *C. difficile*, in contrast with *B. subtilis* for which muramic-δ-lactam–deficient spores have been reported to induce no modification of sporulation (22).

In *C. difficile*, mutants affected for germination have either a strongly reduced virulence or no virulence in hamster models. In our study, the *pdaA1* mutant strain has a significant delay in virulence, but eventually it reaches a mortality similar to the parental strain. This delay in virulence could be explained by a delayed germination of the *pdaA1* mutant *in vivo*. In Syrian hamsters, *C. difficile* spores have been shown to germinate within the 1st h in the small intestine (43). However, spores have been shown to be involved in the first steps of colonization, through adhesion to the host mucus (9). This suggests that *pdaA1* mutant spores may not be fully cleared from the gastrointestinal tract and therefore establish infection. However, the delay in germination might change the location in which spores germinate. Among *C. difficile* isolates, lower germination efficiency was correlated to a more severe CDI in mice (44), and the authors suggested that a slight change in germination location within the host may change the severity of the infection. In this study, the potential change in germination location does not alter *C. difficile* virulence.

Table 2
Strains and plasmids
References 40, 51, and 55 are cited in the table.

Name	Characteristics	Reference
Bacterial strains		
Escherichia coli		
TG1	*E. coli* k12 (F', *tra* D36, *lacIq*, Δ*lacZ*, MIS, *pro* A+B+/SupE, Δ(*hdsM-mcrB*))	Laboratory
HB101pRK24	*E. coli* (pRK24) (F - Δ(*gpt-proA*) 62 Leu B6 *gln* V44 *ara*-14 *gal*K2 *lac*Y1 Δ(*mcrC-mrr*) *rps* L20 (*srt*^{r}) *xyl*-5 *mlt*-1 *rec* A13, pRK24)	Laboratory
Clostridium difficile		
630Δ*erm*	Erythromycin sensitive 630 derived strain	(51)
630Δ*erm* Δ14300, *pdaA1* mutant	ΔCD630_14300 derivative of 630Δ*erm* strain	This work
630Δ*erm* Δ27190, *pdaA2* mutant	ΔCD630_27190 derivative of 630Δ*erm* strain	This work
630Δ*erm* Δ27190Δ14300	ΔCD630_14300 derivative of 630Δ*erm* Δ27190 (*pdaA2*) mutant	This work
630Δ*erm*(pMTL84151)	630Δ*erm* strain carrying the empty control plasmid pMTL84151	This work
630Δ*erm*Δ14300(pMTL84151)	Δ*pdaA1* mutant strain carrying the empty control plasmid pMTL84151	This work
630Δ*erm*Δ14300(pCH67)	Δ*pdaA1* mutant strain carrying the complementation plasmid pCH67	This work
Plasmids and vectors		
pBLUNT	Linear cloning vector, blunt extremities, lacAα-ccdB, MCS,T7 promotor, kanamycin resistance, pUC origin	Invitrogen
pMTL-SC7315	Circular cloning vector, 6000 nucleotides, c*atP, codA*,	(55)
pMTL-84151	Circular cloning vector, 6300 nucleotides, *catP*, α*LacZ*.	(40)
pMB4	pMTLSC7315 derived CPEC assembly of homologous regions for the deletion of CD630_27190	This work
pMB5	pMTLSC7315 derived CPEC assembly of homologous regions for the deletion of CD630_14300	This work
pCH66	pBLUNT derived traditional cloning of insert 94 for *pdaA1* complementation	This work
pCH67	pCH66 subcloning for *pdaA1* complementation, pMTL84151 derived	This work

In CDI, spores are responsible for both infection and dissemination, and intestinal sporulation may have a role in virulence (45). A better sporulation *in vitro* has been correlated to a more severe CDI (46). The *pdaA1* mutant is impaired in sporulation and may therefore have a lower dissemination rate in the environment and may be less susceptible to promote CDI. The *N*-deacetylase inhibitors are beginning to be investigated (47–50), and one of them may inhibit PdaA1. Inhibiting this *N*-deacetylase, probably in combination with other potential targets, may allow us to reduce sporulation, decrease spore heat resistance, slow germination, and therefore impair *C. difficile* virulence and dissemination capability.

In summary, we showed that muramic-δ-lactams have a much broader impact in *C. difficile* than initially described in *B. subtilis* and constitute a novel factor linking both the germination and sporulation processes as well as spore heat resistance. Our study adds a significant contribution in the recent efforts to characterize germination and CDI pathogenesis. It provides an insight into a new strategy to target *C. difficile* and its dissemination by targeting enzymes involved in cortex synthesis.

Experimental procedures

Bacterial strains and plasmids

Plasmids and strains used in this study can be found in Table 2. The *C. difficile* strains are all isogenic derivatives of the 630Δ*erm* strain (51), an erythromycin-sensitive derivative of the clinical 630 strain (52). *Escherichia coli* was grown aerobically at 37 °C in LB medium, supplemented with ampicillin (100 μg/ml), kanamycin (40 μg/ml), and chloramphenicol (25 μg/ml) as needed. *C. difficile* was routinely grown in brain–heart infusion medium (BHI, BD Biosciences) sporulation medium (SM, as described previously (33)) or SMC medium (39, 53). Mutant selection steps of the allelic exchange mutagenesis were carried out on *C. difficile* minimal medium (CDMM (54)). Media were supplemented with thiamphenicol (Thi, 15 μg/ml), 0.1% sodium taurocholate (Sigma), 1% defibrinated horse blood, or "*C. difficile*-selective supplement" (25% (w/v) D-cycloserine, 0.8% (w/v) cefoxitin; OXOID) when required. Cultures of *C. difficile* were carried out at 37 °C in an anaerobic chamber (Jacomex, 5% H_2–5% CO_2–90% N_2).

Molecular biology

Plasmid extractions and DNA purifications were carried using the QIAPrep Spin Miniprep kit (Qiagen) and E.Z.N.A. Cycle Pure kit (Omega), respectively, according to the manufacturer's instructions. PCRs were carried out using either the high-fidelity Phusion DNA polymerase (ThermoFisher Scientific) for cloning and screening of *C. difficile* or the *Taq*DNA polymerase (New England Biolabs) from screening steps in *E. coli*. Restriction enzymes were used according the manufacturer's instructions.

Construction of mutants and complemented strains

Genes of interest were deleted in the 630Δ*erm* strain using the allelic exchange mutagenesis protocol as described previously (55). Plasmids used for the mutagenesis were built using a one-step seamless cloning method, the circular polymerase extension cloning (56). For each desired mutant, DNA fragments were designed to contain 1200-bp sequences of either upstream or downstream CD630_14300 and CD630_27190 as well as overlapping regions between the vector of choice and DNA fragments (Table S6). These regions were designed to delete the gene of interest, starting from the RBS to the STOP codon. Homologous regions for deletion of CD630_14300 and CD630_27190 were amplified from *C. difficile* 630Δ*erm* genomic DNA using hybrid primers HC174/HC176 and HC175/HC177, giving rise to two 1220-bp DNA fragments. Similarly, homologous regions for CD630_27190 in-frame deletion were amplified using hybrid primers HC185/HC187 and HC186/HC188, giving rise to 1200- and 1230-bp DNA fragments. For circular polymerase extension cloning, the pMTLSC7315 cloning vector was amplified using 7315A/7315B primers, producing a 6000-bp linearized vector. After purification, each set of upstream and downstream DNA fragments was combined with the linearized pMTLSC7315 vector in a 1:1 to 2:1 molar ratio of insert-to-vector and processed in the specific PCR amplification program recommended (56, 57), producing double-stranded circular plasmids that were directly transformed into competent *E. coli* TG1 cells. The two pairs of homologous regions for CD630_14300 and CD630_27190 deletion, respectively, cloned into the linearized pMTLSC7315 vector gave rise to pMB5 and pMB4. Inserts were sequenced to confirm the absence of mutations in the inserts of both plasmids.

The CD630_14300 and CD630_27190 genes were deleted using the allelic exchange method. The recombinant pMB5 plasmid was transformed into *E. coli* HB101(pRK24) and then introduced into *C. difficile* 630Δ*erm* strain by heterogramic conjugation, selecting for thiamphenicol resistance. Using the protocol described previously (55), single crossover events were screened using HC177/HC178 and HC174/HC179 primer sets. Colonies corresponding to single crossover events were selected and further processed for selection of the second crossover event. Clones obtained on CDMM medium supplemented with 5-fluorocytosine were streaked onto BHI and BHI supplemented with thiamphenicol. Thi^S clones were then screened with HC178/HC179 to detect which clones corresponded to the desired gene deletion. Using these primers, clones producing a 3560-bp DNA fragment were considered as parental revertants, and clones producing a 2700-bp DNA fragment were isolated and considered as mutants. Similarly, for CD630_27190 deletion, single crossover events were screened using HC188/HC189 and HC185/HC190, and FC^R Thi^S clones were screened for the second crossover event using HC189/HC190. Clones producing a 3550-bp amplification using these primers were considered as parental revertants, and clones producing a 2540-bp amplification were isolated and considered as mutants. To obtain the double mutant ΔCD630_27190, the same method was applied, introducing the deletion of ΔCD630_14300 in the ΔCD630_27190 mutant.

The complementation plasmid for *pdaA1* was built using traditional restriction cloning methods as follows: the full-length sequence of CD630_14300 plus 330 bp upstream was PCR-amplified from *C. difficile* 630Δ*erm* genomic DNA using HC254/HC272 (Table S6), and the 1240-bp product was ligated into the pBLUNT linear vector from the Zero Blunt PCR cloning kit (Invitrogen), giving rise to pCH66. After sequencing, the pCH66 construct and the pMTL84151 definitive vector were digested using KpnI and XbaI, and the 1.3-kb KpnI/XbaI DNA sequence extracted from pCH66 was ligated with the linearized pMTL84151, giving rise to the final construct pCH67. The recombinant pCH67 plasmid was transformed into *E. coli* HB101(pRK24) and then introduced into *C. difficile* Δ*pdaA1* strain by heterogramic conjugation, selecting for thiamphenicol resistance. Similarly, 630Δ*erm* and Δ*pdaA1* mutant strains received the pMTL84151 empty plasmid as a control.

Spore preparation

Spore preparations for the germination assays, resistance assays, TEM spore measurements, and the *in vivo* virulence study were obtained according to an adapted protocol described previously (39). Briefly, *C. difficile* was grown for 16 h in SMC broth and plated in the morning onto SMC agar plates. Plates were incubated at 37 °C in the anaerobic chamber for up to 7 days, monitoring sporulation regularly. Plates were then harvested in water, washed twice, and then left at 4 °C for 2–7 days. Spore suspensions were then washed again with water. When pure spore suspensions were needed, a 20–50% HistoDenz gradient was then applied to the suspensions. To remove traces of HistoDenz, suspensions were then washed an additional 10 times with water, and spore preparations were stored at 4 °C. Spore suspension purity was assessed using light microscopy examination as described by Popham *et al.* (16). Spore suspensions were considered pure when they were at least 98% free of contaminating vegetative cells, cell debris, and sporulating cells.

Transmission EM

TEM experiments were conducted on two types of spore preparations. Spores and vegetative cells from the sporulating culture were harvested by centrifugation after 48 h incubation in SMC broth and washed once in PBS. Spore measurements were obtained using the spore preparation protocol described above. Samples were prepared as described in Sadovskaya *et al.* (58). Staining and examinations were done by the GABI-MIMA2 TEM Platform at INRA, Jouy-en-Josas, France. Grids were examined with a Hitachi HT7700 electron microscope operated at 80 kV, and images were acquired with a charge-coupled device camera (AMT).

Spore measurements were conducted as follows: 10 longitudinal and 10 transversal spore cross-sections were selected for the parental and *pdaA1* mutant spores. The core length, core width, and cortex thickness were measured for each section. The protoplast volume (core) and sporoplast volume (core and cortex) were calculated according to Beaman *et al.*: volume = (4/3) π (width/2) × 2× (length/2) (59). The protoplast-to-

sporoplast ratio was calculated by dividing the calculated core volume (protoplast) by the volume of the core plus cortex layer (sporoplast).

Spore cortex extraction

Spore cortex extractions were conducted as described in a protocol for *B. subtilis* (16). Briefly, 5 mg of freeze-dried pure spore preparations (>99%) were hydrated in water for 16 h at 4 °C. Suspensions were treated twice with a decoating buffer (50 mM Tris-HCl, pH 8, 8 M urea, 1% SDS, 50 mM DTT) for 1 h at 37 °C. After being washed five times in water, lytic enzymes were inactivated with 5% TCA during 6 min at 95 °C, and spores were washed in 1 M Tris-HCl and then washed five times in water. Spores were then left for 16 h incubated in a Tris-HCl buffer with trypsin at 37 °C. The treated suspensions were then boiled in 1% SDS for 15 min. Pellets were washed 15 times with water until total elimination of SDS. Peptidoglycan was then digested 16 h with mutanolysin in a sodium phosphate buffer. The suspensions were centrifuged, and muropeptides contained in the supernatant were freeze-dried 16 h (Telstar cryodos). Soluble muropeptides were then mixed with an equal volume of 500 mM borate buffer, pH 9, and reduced with sodium borohydride ($NaBH_4$). After 30 min at room temperature, the pH was adjusted to 3 using orthophosphoric acid (H_3PO_4). After centrifugation, reduced muropeptides were diluted 5-fold in mobile phase (formic acid 0,1% in water).

Muropeptide analysis

Muropeptides were analyzed by UHPLC-HRMS (Unité Biologie et Génétique de la Paroi Bactérienne, Institut Pasteur). A Dionex Ultimate 3000 UHPLC was coupled to a QExactive Focus (ThermoFisher Scientific). Muropeptides were eluted on a Hypersil God C18 aQ (175 Å, 1.9 μm, 2.1 × 150 mm) column. Column temperature was 50 °C, and the injection volume was 10 μl. UHPLC gradient was programmed as follows: solvent A = 0.1% formic acid in water; solvent B = 0.1% formic acid in acetonitrile; glow = 0.2 ml/min; run time = 45 min; gradient 0–15% B in 30 min. Mass spectrometry was set to positive electrospray ionization mode with a scan range from 200 to 3000. Full scan data-dependent acquisition selected the top three most abundant precursor ions for tandem MS by HCD fragmentation. Peaks were selected with the following criteria: peak area threshold = 2,500,000; at least two fragmentation sets; peak intensity >5000. Percentage of each peak was calculated as the ratio of the peak area over the sum areas of all the peaks in Table 1.

Germination assays

Germination was monitored using an optical density monitoring assay, following a protocol adapted from Ref. 60. Biological triplicates were obtained using independent spore preparations and purified as described above. After heat activation at 37 °C for 20 min, germination was measured by monitoring the decrease in optical density of a purified spore suspension following the addition of 0.1% taurocholate as a germinant. Germination was expressed as the ratio between the $OD_{600\ nm}$ at a given time and the initial $OD_{600\ nm}$ of the spore suspension, × 100. In the standard assay, optical density was monitored for an hour. In the extended assay, monitoring was prolonged to 24 h. Germination was also investigated using a solid medium: spore suspensions were prepared by serial dilution, plated onto BHI agar plates supplemented with horse blood and 0.1% taurocholate, and incubated for 48 h at 37 °C in an anaerobic chamber. At 24 and 48 h incubation, plates of the parental strain and *pdaA1* were photographed, and isolated colonies were measured.

Sporulation and spore resistance assays

Sporulation studies and resistance assays were done according to a slightly modified version of the protocol described previously (33). *C. difficile* strains were grown 16 h in SM broth containing the appropriate antibiotics and used to inoculate SM broth to obtain $OD_{600\ nm} = 0.05$. After a 72-h incubation at 37 °C, 1 ml of culture was withdrawn and serially diluted in PBS.

Total cell titers were calculated by plating 100 μl of these untreated dilutions onto BHI plates containing 0.1% taurocholate and the appropriate antibiotics. Ethanol-resistant spore titers were calculated by adding an equal volume of absolute ethanol to 400 μl of the untreated dilutions, incubating for 15 min at room temperature, and finally plating 100 μl of alcohol-treated dilutions onto plates. Heat-resistant spore titers were then calculated by incubating the remaining 400 μl of serial dilutions at 65 °C for 20 min and then plating 100 μl of the appropriate dilutions.

All dilutions were plated onto BHI plates containing taurocholate and the appropriate antibiotics. The percentage of sporulation was determined as the ratio between the number of ethanol-resistant cells/ml and the total number of cells/ml × 100. The percentage of heat-resistant spores was determined as the ratio between heat-resistant titers and ethanol-resistant titers × 100.

For the resistance assay on spores, the log reduction was determined as follows: $\log_{10}$(untreated titers) − $\log_{10}$(treated titers). Spore suspensions of both the parental strain harboring the empty plasmid, the *pdaA1* mutant harboring the empty plasmid, and the complemented *pdaA1* mutant were incubated for 20 min at 37 °C with 2.5% H_2O_2, 50% ethanol, or water as a negative control, followed by serial dilution and plating on BHI agar plates supplemented with 0.1% sodium taurocholate, to allow efficient germination, and the appropriate antibiotics.

In vivo virulence assay

Adult female Syrian golden hamsters were used for the study. Absence of *C. difficile* was monitored after reception of animals and before starting the assay. To induce susceptibility to infection with *C. difficile*, hamsters were treated with antibiotics for 5 days before infection: intraperitoneal injection of clindamycin (0.3 ml, 50 mg/kg) 5 days before infection, and oral administration of gentamycin (0.5 ml, 2.5 mg/kg) twice a day every day for 5 days. Hamsters were infected orally by administration of 5×10^4 spores of either the parental or the *pdaA1* mutant strain. Enumeration of spore suspensions was conducted on solid medium, after 48 h incubation at 37 °C. *C. difficile* presence was monitored through an on/off test: fecal pellets from each hamster were cultured in BHI supplemented with 0.1% sodium taurocholate for 12 h and plated on BHI agar plated supplemented with 25% (w/v) D-cycloserine, 0.8% (w/v) cefoxitin, and 1%

defibrinated horse blood. Typical fluorescent colonies were screened under UV light (312 nm).

Ethics statement

Adult female Syrian golden hamsters (95–105 g, Charles River France) were housed in individual sterile cages in an animal biosafety level 2 facility within the Central Animal Facility of the Pharmacy Faculty, according to European Union guidelines for the handling of laboratory animals, and procedures for infection, euthanasia, and specimen collection were approved by the Ethics Committee CAPSUD (Protocol APAFiS no. 7492-2016101014285698).

Statistics

Statistical analyses, including the Kaplan-Meier survival analysis, were carried out using BiostaTGV, an on-line statistical analysis service based on calculations obtained with the statistics software R. The p value is indicated for all comparisons when differences were found to be statistically significant.

Author contributions—H. C. and T. C. conceptualization; H. C., A. R., and R. W. formal analysis; H. C. and T. C. validation; H. C., A. R., R. W., and T. C. investigation; H. C. and T. C. methodology; H. C. and T. C. writing-original draft; H. C., A. R., R. W., C. J., I. G. B., and T. C. writing-review and editing; C. J. and I. G. B. resources; C. J., I. G. B., and T. C. supervision; T. C. visualization; T. C. project administration.

Acknowledgments—This work has benefited from the facilities and expertise of MIMA2 MET, INRA-UMR GABI. We thank M. Gohar for help and support on this project. M. Bleuzé is acknowledged for technical help in molecular biology.

References

1. Rodriguez Diaz, C., Seyboldt, C., and Rupnik, M. (2018) Non-human *C. difficile* reservoirs and sources: animals, food, environment. *Adv. Exp. Med. Biol.* **1050,** 227–243 CrossRef Medline
2. Zanella Terrier, M. C., Simonet, M. L., Bichard, P., and Frossard, J. L. (2014) Recurrent *Clostridium difficile* infections: the importance of the intestinal microbiota. *World J. Gastroenterol.* **20,** 7416–7423 CrossRef Medline
3. Cohen, S. H., Gerding, D. N., Johnson, S., Kelly, C. P., Loo, V. G., McDonald, L. C., Pepin, J., Wilcox, M. H., Society for Health care Epidemiology of America, and Infectious Diseases Society of America. (2010) Clinical practice guidelines for *Clostridium difficile* infection in adults: 2010 update by the society for health care epidemiology of America (SHEA) and the infectious diseases society of America (IDSA). *Infect. Control Hosp. Epidemiol.* **31,** 431–455 CrossRef Medline
4. Debast, S. B., Bauer, M. P., and Kuijper, E. J. (2014) European Society of Clinical Microbiology and Infectious Diseases: update of the treatment guidance document for *Clostridium difficile* infection. *Clin. Microbiol. Infect.* **20,** Suppl. 2, 1–26 CrossRef Medline
5. Jones, A. M., Kuijper, E. J., and Wilcox, M. H. (2013) *Clostridium difficile*: a European perspective. *J. Infect.* **66,** 115–128 CrossRef Medline
6. Lessa, F. C., Winston, L. G., McDonald, L. C., and Emerging Infections Program C. difficile Surveillance Team. (2015) Burden of *Clostridium difficile* infection in the United States. *N. Engl. J. Med.* **372,** 2369–2370 CrossRef Medline
7. Loo, V. G., Poirier, L., Miller, M. A., Oughton, M., Libman, M. D., Michaud, S., Bourgault, A. M., Nguyen, T., Frenette, C., Kelly, M., Vibien, A., Brassard, P., Fenn, S., Dewar, K., Hudson, T. J., *et al.* (2005) A predominantly clonal multi-institutional outbreak of *Clostridium difficile*-associated diarrhea with high morbidity and mortality. *N. Engl. J. Med.* **353,** 2442–2449 CrossRef Medline
8. Deakin, L. J., Clare, S., Fagan, R. P., Dawson, L. F., Pickard, D. J., West, M. R., Wren, B. W., Fairweather, N. F., Dougan, G., and Lawley, T. D. (2012) The *Clostridium difficile spo0A* gene is a persistence and transmission factor. *Infect. Immun.* **80,** 2704–2711 CrossRef Medline
9. Hong, H. A., Ferreira, W. T., Hosseini, S., Anwar, S., Hitri, K., Wilkinson, A. J., Vahjen, W., Zentek, J., Soloviev, M., and Cutting, S. M. (2017) The spore coat protein CotE facilitates host colonization by *Clostridium difficile*. *J. Infect. Dis.* **216,** 1452–1459 CrossRef Medline
10. Setlow, P. (2014) Spore resistance properties. *Microbiol. Spectrum* **2**
11. Leggett, M. J., McDonnell, G., Denyer, S. P., Setlow, P., and Maillard, J. Y. (2012) Bacterial spore structures and their protective role in biocide resistance. *J. Appl. Microbiol.* **113,** 485–498 CrossRef Medline
12. Setlow, P. (2006) Spores of *Bacillus subtilis*: their resistance to and killing by radiation, heat and chemicals. *J. Appl. Microbiol.* **101,** 514–525 CrossRef Medline
13. Ghosh, S., Setlow, B., Wahome, P. G., Cowan, A. E., Plomp, M., Malkin, A. J., and Setlow, P. (2008) Characterization of spores of *Bacillus subtilis* that lack most coat layers. *J. Bacteriol.* **190,** 6741–6748 CrossRef Medline
14. Permpoonpattana, P., Phetcharaburanin, J., Mikelsone, A., Dembek, M., Tan, S., Brisson, M. C., La Ragione, R., Brisson, A. R., Fairweather, N., Hong, H. A., and Cutting, S. M. (2013) Functional characterization of *Clostridium difficile* spore coat proteins. *J. Bacteriol.* **195,** 1492–1503 CrossRef Medline
15. Loshon, C. A., Genest, P. C., Setlow, B., and Setlow, P. (1999) Formaldehyde kills spores of *Bacillus subtilis* by DNA damage and small, acid-soluble spore proteins of the α/β-type protect spores against this DNA damage. *J. Appl. Microbiol.* **87,** 8–14 CrossRef Medline
16. Popham, D. L., Helin, J., Costello, C. E., and Setlow, P. (1996) Analysis of the peptidoglycan structure of *Bacillus subtilis* endospores. *J. Bacteriol.* **178,** 6451–6458 CrossRef Medline
17. Atrih, A., and Foster, S. J. (2001) Analysis of the role of bacterial endospore cortex structure in resistance properties and demonstration of its conservation amongst species. *J. Appl. Microbiol.* **91,** 364–372 CrossRef Medline
18. Orsburn, B., Melville, S. B., and Popham, D. L. (2008) Factors contributing to heat resistance of *Clostridium perfringens* endospores. *Appl. Environ. Microbiol.* **74,** 3328–3335 CrossRef Medline
19. Fukushima, T., Yamamoto, H., Atrih, A., Foster, S. J., and Sekiguchi, J. (2002) A polysaccharide deacetylase gene (*pdaA*) is required for germination and for production of muramic δ-lactam residues in the spore cortex of *Bacillus subtilis*. *J. Bacteriol.* **184,** 6007–6015 CrossRef Medline
20. Sekiguchi, J., Akeo, K., Yamamoto, H., Khasanov, F. K., Alonso, J. C., and Kuroda, A. (1995) Nucleotide sequence and regulation of a new putative cell wall hydrolase gene, *cwlD*, which affects germination in *Bacillus subtilis*. *J. Bacteriol.* **177,** 5582–5589 CrossRef Medline
21. Gilmore, M. E., Bandyopadhyay, D., Dean, A. M., Linnstaedt, S. D., and Popham, D. L. (2004) Production of muramic δ-lactam in *Bacillus subtilis* spore peptidoglycan. *J. Bacteriol.* **186,** 80–89 CrossRef Medline
22. Popham, D. L., Helin, J., Costello, C. E., and Setlow, P. (1996) Muramic lactam in peptidoglycan of *Bacillus subtilis* spores is required for spore outgrowth but not for spore dehydration or heat resistance. *Proc. Natl. Acad. Sci. U.S.A.* **93,** 15405–15410 CrossRef Medline
23. Fukushima, T., Kitajima, T., and Sekiguchi, J. (2005) A polysaccharide deacetylase homologue, PdaA, in *Bacillus subtilis* acts as an *N*-acetylmuramic acid deacetylase *in vitro*. *J. Bacteriol.* **187,** 1287–1292 CrossRef Medline
24. Hu, K., Yang, H., Liu, G., and Tan, H. (2006) Identification and characterization of a polysaccharide deacetylase gene from *Bacillus thuringiensis*. *Can. J. Microbiol.* **52,** 935–941 CrossRef Medline
25. Fimlaid, K. A., and Shen, A. (2015) Diverse mechanisms regulate sporulation σ factor activity in the Firmicutes. *Curr. Opin. Microbiol.* **24,** 88–95 CrossRef Medline
26. Gil, F., Lagos-Moraga, S., Calderón-Romero, P., Pizarro-Guajardo, M., and Paredes-Sabja, D. (2017) Updates on *Clostridium difficile* spore biology. *Anaerobe* **45,** 3–9 CrossRef Medline
27. Paredes-Sabja, D., Shen, A., and Sorg, J. A. (2014) *Clostridium difficile* spore biology: sporulation, germination, and spore structural proteins. *Trends Microbiol.* **22,** 406–416 CrossRef Medline

28. Peltier, J., Courtin, P., El Meouche, I., Lemée, L., Chapot-Chartier, M. P., and Pons, J. L. (2011) *Clostridium difficile* has an original peptidoglycan structure with a high level of *N*-acetylglucosamine deacetylation and mainly 3-3 cross-links. *J. Biol. Chem.* **286,** 29053–29062 CrossRef Medline
29. Sievers, F., Wilm, A., Dineen, D., Gibson, T. J., Karplus, K., Li, W., Lopez, R., McWilliam, H., Remmert, M., Söding, J., Thompson, J. D., and Higgins, D. G. (2011) Fast, scalable generation of high-quality protein multiple sequence alignments using Clustal Omega. *Mol. Syst. Biol.* **7,** 539 Medline
30. Yu, N. Y., Wagner, J. R., Laird, M. R., Melli, G., Rey, S., Lo, R., Dao, P., Sahinalp, S. C., Ester, M., Foster, L. J., and Brinkman, F. S. (2010) PSORTb 3.0: improved protein subcellular localization prediction with refined localization subcategories and predictive capabilities for all prokaryotes. *Bioinformatics* **26,** 1608–1615 CrossRef Medline
31. de Castro, E., Sigrist, C. J., Gattiker, A., Bulliard, V., Langendijk-Genevaux, P. S., Gasteiger, E., Bairoch, A., and Hulo, N. (2006) ScanProsite: detection of PROSITE signature matches and ProRule-associated functional and structural residues in proteins. *Nucleic Acids Res.* **34,** W362–W365 CrossRef Medline
32. Lawley, T. D., Croucher, N. J., Yu, L., Clare, S., Sebaihia, M., Goulding, D., Pickard, D. J., Parkhill, J., Choudhary, J., and Dougan, G. (2009) Proteomic and genomic characterization of highly infectious *Clostridium difficile* 630 spores. *J. Bacteriol.* **191,** 5377–5386 CrossRef Medline
33. Pereira, F. C., Saujet, L., Tomé, A. R., Serrano, M., Monot, M., Couture-Tosi, E., Martin-Verstraete, I., Dupuy, B., and Henriques, A. O. (2013) The spore differentiation pathway in the enteric pathogen *Clostridium difficile*. *PLoS Genet.* **9,** e1003782 CrossRef Medline
34. Atrih, A., Bacher, G., Körner, R., Allmaier, G., and Foster, S. J. (1999) Structural analysis of *Bacillus megaterium* KM spore peptidoglycan and its dynamics during germination. *Microbiology* **145,** 1033–1041 CrossRef Medline
35. Fukushima, T., Tanabe, T., Yamamoto, H., Hosoya, S., Sato, T., Yoshikawa, H., and Sekiguchi, J. (2004) Characterization of a polysaccharide deacetylase gene homologue (*pdaB*) on sporulation of *Bacillus subtilis*. *J. Biochem.* **136,** 283–291 CrossRef Medline
36. Markowitz, V. M., Chen, I. M., Palaniappan, K., Chu, K., Szeto, E., Grechkin, Y., Ratner, A., Jacob, B., Huang, J., Williams, P., Huntemann, M., Anderson, I., Mavromatis, K., Ivanova, N. N., and Kyrpides, N. C. (2012) IMG: the Integrated Microbial Genomes database and comparative analysis system. *Nucleic Acids Res.* **40,** D115–D122 CrossRef Medline
37. Janoir, C., Denève, C., Bouttier, S., Barbut, F., Hoys, S., Caleechum, L., Chapetón-Montes, D., Pereira, F. C., Henriques, A. O., Collignon, A., Monot, M., and Dupuy, B. (2013) Adaptive strategies and pathogenesis of *Clostridium difficile* from *in vivo* transcriptomics. *Infect. Immun.* **81,** 3757–3769 CrossRef Medline
38. Saujet, L., Pereira, F. C., Serrano, M., Soutourina, O., Monot, M., Shelyakin, P. V., Gelfand, M. S., Dupuy, B., Henriques, A. O., and Martin-Verstraete, I. (2013) Genome-wide analysis of cell type-specific gene transcription during spore formation in *Clostridium difficile*. *PLoS Genet.* **9,** e1003756 CrossRef Medline
39. Dembek, M., Stabler, R. A., Witney, A. A., Wren, B. W., and Fairweather, N. F. (2013) Transcriptional analysis of temporal gene expression in germinating *Clostridium difficile* 630 endospores. *PLoS One* **8,** e64011 CrossRef Medline
40. Heap, J. T., Pennington, O. J., Cartman, S. T., and Minton, N. P. (2009) A modular system for *Clostridium shuttle* plasmids. *J. Microbiol. Methods* **78,** 79–85 CrossRef Medline
41. Heffron, J. D., Sherry, N., and Popham, D. L. (2011) *In vitro* studies of peptidoglycan binding and hydrolysis by the *Bacillus anthracis* germination-specific lytic enzyme SleB. *J. Bacteriol.* **193,** 125–131 CrossRef Medline
42. Wu, X., Grover, N., Paskaleva, E. E., Mundra, R. V., Page, M. A., Kane, R. S., and Dordick, J. S. (2015) Characterization of the activity of the spore cortex lytic enzyme CwlJ1. *Biotechnol. Bioeng.* **112,** 1365–1375 CrossRef Medline
43. Wilson, K. H., Sheagren, J. N., and Freter, R. (1985) Population dynamics of ingested *Clostridium difficile* in the gastrointestinal tract of the Syrian hamster. *J. Infect. Dis.* **151,** 355–361 CrossRef Medline
44. Carlson, P. E., Jr, Walk, S. T., Bourgis, A. E., Liu, M. W., Kopliku, F., Lo, E., Young, V. B., Aronoff, D. M., and Hanna, P. C. (2013) The relationship between phenotype, ribotype, and clinical disease in human *Clostridium difficile* isolates. *Anaerobe* **24,** 109–116 CrossRef Medline
45. Dembek, M., Willing, S. E., Hong, H. A., Hosseini, S., Salgado, P. S., and Cutting, S. M. (2017) Inducible Expression of *spo0A* as a Universal Tool for Studying Sporulation in *Clostridium difficile*. *Front. Microbiol.* **8,** 1793 CrossRef Medline
46. Carlson, P. E., Jr., Kaiser, A. M., McColm, S. A., Bauer, J. M., Young, V. B., Aronoff, D. M., and Hanna, P. C. (2015) Variation in germination of *Clostridium difficile* clinical isolates correlates to disease severity. *Anaerobe* **33,** 64–70 CrossRef Medline
47. Ariyakumaran, R., Pokrovskaya, V., Little, D. J., Howell, P. L., and Nitz, M. (2015) Direct Staudinger-phosphonite reaction provides methylphosphonamidates as inhibitors of CE4 de-*N*-acetylases. *Chembiochem* **16,** 1350–1356 CrossRef Medline
48. Chibba, A., Poloczek, J., Little, D. J., Howell, P. L., and Nitz, M. (2012) Synthesis and evaluation of inhibitors of *E. coli* PgaB, a polysaccharide de-*N*-acetylase involved in biofilm formation. *Org. Biomol. Chem.* **10,** 7103–7107 CrossRef Medline
49. Hall, R. S., Brown, S., Fedorov, A. A., Fedorov, E. V., Xu, C., Babbitt, P. C., Almo, S. C., and Raushel, F. M. (2007) Structural diversity within the mononuclear and binuclear active sites of *N*-acetyl-D-glucosamine-6-phosphate deacetylase. *Biochemistry* **46,** 7953–7962 CrossRef Medline
50. Murphy-Benenato, K. E., Olivier, N., Choy, A., Ross, P. L., Miller, M. D., Thresher, J., Gao, N., and Hale, M. R. (2014) Synthesis, structure, and SAR of tetrahydropyran-based LpxC inhibitors. *ACS Med. Chem. Lett.* **5,** 1213–1218 CrossRef Medline
51. Hussain, H. A., Roberts, A. P., and Mullany, P. (2005) Generation of an erythromycin-sensitive derivative of *Clostridium difficile* strain 630 (630Delta*erm*) and demonstration that the conjugative transposon *Tn916*DeltaE enters the genome of this strain at multiple sites. *J. Med. Microbiol.* **54,** 137–141 CrossRef Medline
52. Sebaihia, M., Wren, B. W., Mullany, P., Fairweather, N. F., Minton, N., Stabler, R., Thomson, N. R., Roberts, A. P., Cerdeño-Tarraga, A. M., Wang, H., Holden, M. T., Wright, A., Churcher, C., Quail, M. A., Baker, S., *et al.* (2006) The multidrug-resistant human pathogen *Clostridium difficile* has a highly mobile, mosaic genome. *Nat. Genet.* **38,** 779–786 CrossRef Medline
53. Permpoonpattana, P., Hong, H. A., Phetcharaburanin, J., Huang, J. M., Cook, J., Fairweather, N. F., and Cutting, S. M. (2011) Immunization with *Bacillus* spores expressing toxin A peptide repeats protects against infection with *Clostridium difficile* strains producing toxins A and B. *Infect. Immun.* **79,** 2295–2302 CrossRef Medline
54. Cartman, S. T., and Minton, N. P. (2010) A mariner-based transposon system for *in vivo* random mutagenesis of *Clostridium difficile*. *Appl. Environ. Microbiol.* **76,** 1103–1109 CrossRef Medline
55. Cartman, S. T., Kelly, M. L., Heeg, D., Heap, J. T., and Minton, N. P. (2012) Precise manipulation of the *Clostridium difficile* chromosome reveals a lack of association between the *tcdC* genotype and toxin production. *Appl. Environ. Microbiol.* **78,** 4683–4690 CrossRef Medline
56. Quan, J., and Tian, J. (2011) Circular polymerase extension cloning for high-throughput cloning of complex and combinatorial DNA libraries. *Nat. Protoc.* **6,** 242–251 CrossRef Medline
57. Quan, J., and Tian, J. (2014) Circular polymerase extension cloning. *Methods Mol. Biol.* **1116,** 103–117 CrossRef Medline
58. Sadovskaya, I., Vinogradov, E., Courtin, P., Armalyte, J., Meyrand, M., Giaouris, E., Palussiere, S., Furlan, S., Pechoux, C., Ainsworth, S., Mahony, J., van Sinderen, D., Kulakauskas, S., Guerardel, Y., and Chapot-Chartier, M. P. (2017) Another brick in the wall: a Rhamnan polysaccharide trapped inside peptidoglycan of *Lactococcus lactis*. *mBio* **8,** e01307-17 CrossRef Medline
59. Beaman, T. C., Greenamyre, J. T., Corner, T. R., Pankratz, H. S., and Gerhardt, P. (1982) Bacterial spore heat resistance correlated with water content, wet density, and protoplast/sporoplast volume ratio. *J. Bacteriol.* **150,** 870–877 Medline
60. Donnelly, M. L., Fimlaid, K. A., and Shen, A. (2016) Characterization of *Clostridium difficile* spores lacking either SpoVAC or dipicolinic acid synthetase. *J. Bacteriol.* **198,** 1694–1707 CrossRef Medline